EXPERIMENTAL STUDY OF TURBULENCE MANIPULATION IN STEPPED SPILLWAYS. IMPLICATIONS ON FLOW RESISTANCE IN SKIMMING FLOWS

CARLOS A. GONZALEZ [1] and HUBERT CHANSON [1]

[1]Dept of Civil Engineering, The University of Queensland, Brisbane QLD 4072, Australia
(Tel: +61-7-3365-4163, Fax: +61-7-3365-4599, e-mail: h.chanson@uq.edu.au)

Abstract

Current expertise in air-water turbulent flows on stepped chutes is limited to laboratory experiments at low to moderate Reynolds numbers on flat horizontal steps. In this study, highly turbulent air-water flows skimming down a large-size stepped chute were systematically investigated with a 22º slope. Turbulence manipulation was conducted using vanes or longitudinal ribs to enhance interactions between skimming flows and cavity recirculating regions. Systematic experiments were performed with seven configurations. The results demonstrated the strong influence of vanes on the air-water flow. An increase in flow resistance was observed consistently with maximum flow resistance achieved with vanes placed in a zigzag pattern.

Keywords: Stepped spillway; Flow resistance; Turbulence; Turbulence manipulation; Air entrainment; Physical modelling

1. INTRODUCTION

Numerous studies of stepped spillway flows were conducted with different approaches over the past forty years. Pertinent reviews include Chanson (2001), Mossa et al. (2004) and Ohtsu et al. (2004). Only a limited number of published papers refer to highly turbulent flows associated with strong free-surface aeration (e.g. Chanson and Toombes 2002, Yasuda and Chanson 2003). Stepped chute design is common for overflow spillways of gravity and embankment dams. Most structures are designed with flat horizontal steps but some included devices to enhance energy dissipation (Andre et al. 2004, Chanson and Gonzalez 2004). Modern stepped spillways are designed to operate with a skimming flow regime. In a skimming flow, the waters run down the stepped channel as a coherent stream skimming over the pseudo-bottom zones formed by step edges. Beneath cavity recirculation is maintained through the transmission of momentum from the main stream (Fig. 1). There may be some analogy between skimming flows over stepped spillways and skimming flows above large roughness elements, including boundary layer flows past d-type roughness (e.g. Chanson et al. 2002, Djenidi et al. 1999). A pertinent study by Mochizuki et al (1996) investigated turbulent boundary layer past d-type roughness with thin longitudinal ribs. Despite conflicting interpretations of their data, their experiments demonstrated some turbulence manipulation by interfering with the recirculation vortices.

This paper presents the result of a systematic investigation into the effects of several vane configurations on the skimming flow properties. The experiments were conducted in a large stepped channel operating with Reynolds numbers between 4 and 8 E+5. One configuration had flat horizontal steps while 6 others were equipped with vane arrangements (Fig. 2, Table 1). Interactions between free surface and cavity recirculation, turbulence manipulation and flow resistance were systematically investigated for several discharges.

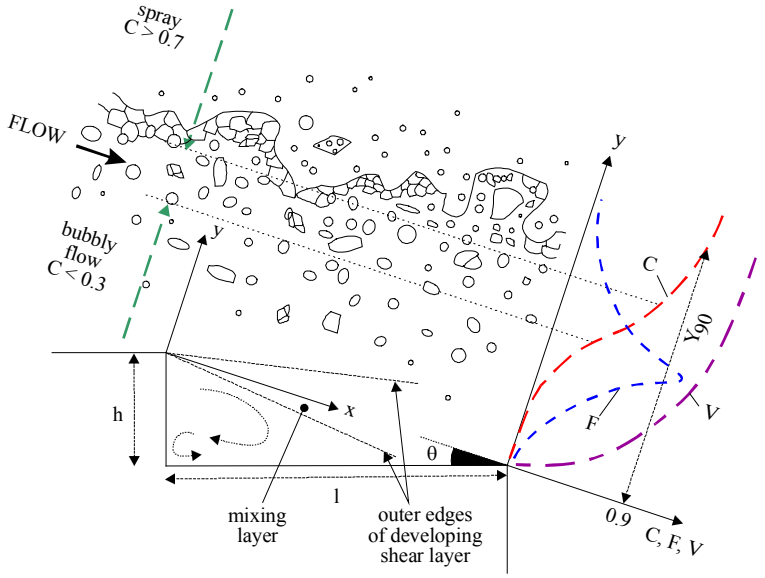

Fig. 1 Sketch of skimming flows down a moderate-slope stepped spillway

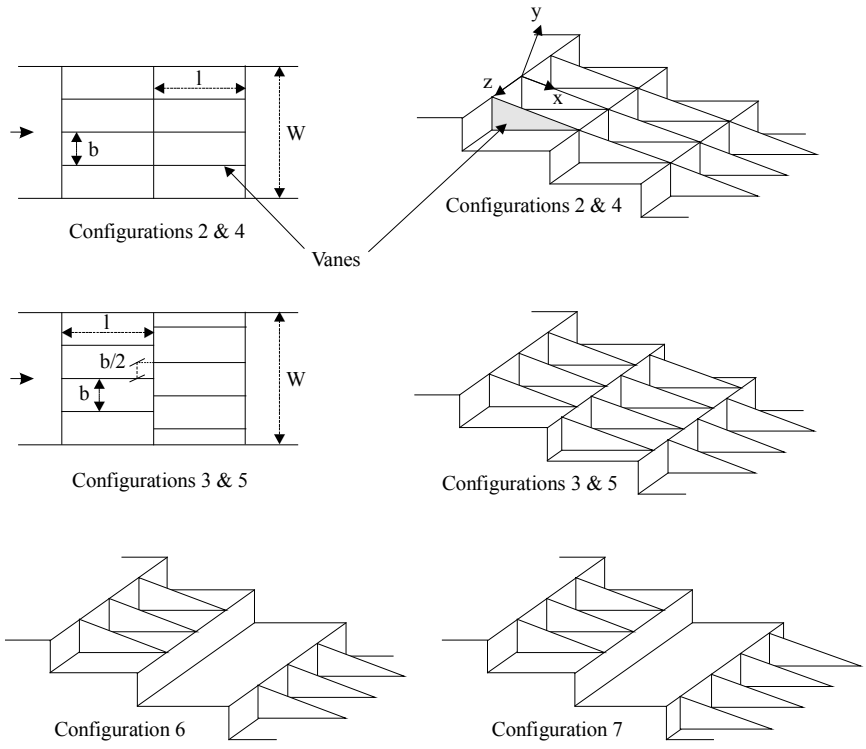

Fig. 2 Sketch of the vanes configurations

2. EXPERIMENTAL FACILITIES

New experiments were conducted at the University of Queensland in a 3.6 m long, 1 m wide, 21.8º slope chute with flow rates ranging from 0.10 to 0.19 m^3/s corresponding to a skimming flow regime (Table 1). The water supply pump was controlled by an adjustable frequency AC motor drive. This enabled for an accurate control of the closed circuit system. Waters were fed from a large basin (1.5 m deep, surface area 6.8 m × 4.8 m) leading to a sidewall convergent with a 4.8:1 contraction ratio. The test section was a broad-crested weir (1 m wide, 0.6 m long, with upstream rounded corner (0.057 m radius) followed by ten identical steps (h = 0.1 m, l = 0.25 m) made of marine ply. The stepped chute was 1 m wide with perspex sidewalls followed by a horizontal concrete-invert canal ending in a dissipation pit.

Herein seven stepped geometries were tested systematically with several flow rates. The first configuration had ten identical flat horizontal steps (Configuration 1). That geometry was similar to that studied by Chanson and Toombes (2002). Experimental observations highlighted the three-dimensional nature of recirculation vortices in the step cavities. In absence of vane (see below), three to four cavity recirculation cells were observed across the 1-m wide channel. These recirculation vortices were believed to be related to longitudinal (streamwise) coherent structures in the mainstream flow. In the second, third, fourth, fifth, sixth and seventh configurations, vanes or longitudinal ribs were placed across the step cavity from steps 2 to 10 as illustrated in Fig. 2. The triangular vanes (0.1 m × 0.25 m) were made of aluminium, although few were made in perspex for flow visualisation next to the sidewall. They did not interfere with the free-stream. The second and fourth configurations had respectively 3 and 7 vanes placed in line. The third and fifth configurations had respectively 3 and 7 vanes placed in zigzag. The sixth configurations had 7 vanes per step set in line every two steps, while the seventh configuration consisted of 7 vanes per step set in a zigzag pattern every two steps. For each configuration, measurements were repeated systematically at each step edge downstream of the inception point of free-surface aeration, at several longitudinal positions between adjacent step edges (i.e. above recirculation cavity) and at several transverse positions for several flow rates. A total of more than 240 vertical profiles were recorded with a minimum of 25 measurement points per profile. Further details on the experiments were reported in Gonzalez (2005).

Table 1. Detailed experimental investigations of turbulence manipulation in skimming flows on moderate slope stepped chutes

Reference	θ deg.	q_W m^2/s	h m	Re	Instrumentation	Geometry
Present Study	21.8	0.10 to 0.19	0.1	4E+5 to 8E+5	Double-tip conductivity probe (∅ = 0.025 mm)	L = 3.3 m. W = 1 m. Uncontrolled broad-crest.
Configuration 1						b = W = 1 m (no vane).
Configuration 2						b = W/4 = 0.25 m (3 vanes in line).
Configuration 3						b = W/4 = 0.25 m (3 vanes in zigzag).
Configuration 4						b = W/8 = 0.125 m (7 vanes in line).
Configuration 5						b = W/8 = 0.125 m (7 vanes in zigzag).
Configuration 6						b = W/8 = 0.125 m (7 vanes in line, every 2 steps).
Configuration 7						b = W/8 = 0.125 m (7 vanes in line, every two steps).

2.1 INSTRUMENTATION AND DATA PROCESSING

Clear-water flow depths were measured with a point gauge. The flow rate was deduced from the measured upstream head above crest, after a detailed in-situ calibration (Gonzalez 2005). Air-water flow properties were recorded with a double-tip conductivity probe (∅ = 0.025 mm) previously used by Chanson and Toombes (2002), Yasuda and Chanson (2003), and Gonzalez and Chanson (2004a). The probe sensors were aligned in the flow direction. The leading tip had a small frontal area (i.e. 0.05 mm^2) and the trailing tip was offset to avoid wake disturbance from the first tip. An air bubble detector (UQ82.518) excited the probe. Its output signal was scanned at 20 kHz for 20 s per probe tip. The translation of the probes normal to the flow direction was controlled by a fine adjustment travelling mechanism connected to a Mitutoyo™ digimatic scale unit. The error on the vertical position of the probe was less than 0.025 mm. The accuracy on the longitudinal probe position was estimated as Δx < +/- 0.5 cm. The accuracy on the transverse position of the probe was less than 1 mm. Flow visualisations were conducted with high-shutter speed digital still and video cameras.

The basic probe outputs were the void fraction, bubble count rate, velocity, turbulence intensity and air/water chord size distributions. The void fraction C is the proportion of time that the probe tip is in the air. The bubble count rate F is the number of bubbles impacting the probe tip per second. With a dual-tip probe design, the velocity measurement is based upon the successive detection of air-water interfaces by the two tips. Herein the velocity was calculated using a cross-correlation technique (e.g. Crowe et al. 1998). The turbulence level Tu was derived from the broadening of the cross-correlation function compared to the auto-correlation function (Chanson and Toombes 2002). Physically, a thin, narrow cross-correlation function corresponds to little fluctuations in interfacial velocity, hence a small turbulence level. The turbulence level Tu is not a point measurement but some spatial average between probe sensors. In low volume fractions, it is equal to the turbulence intensity u'/V. Chord sizes were calculated from the raw probe signal outputs. The results provided a complete characterisation of the streamwise distribution of air and water chords.

3. FLOW OBSERVATIONS

Skimming flows looked similar to self-aerated flows down smooth chutes. At the upstream end, the flow was smooth and transparent. When the outer edge of the developing bottom boundary layer reached the free surface, turbulence induced strong aeration. Downstream of the point of inception of air entrainment, the air-water flow became fully developed and strong exchanges of air-water and momentum occurred between the main stream and the atmosphere. Intense cavity recirculation was observed also below the pseudo-invert formed by the step edges. The air-water flow mixture consisted of a bubbly region (C < 30%), a spray region (C > 70%) and an intermediate zone in between (Fig. 1). Three-dimensional cavity vortices developed beneath the pseudo-bottom formed by the step edges and recirculation was maintained through the transmission of momentum from the main stream. Small-scale vorticity was also generated at the corner of the steps. Skimming flows were characterised by very significant form losses and momentum transfer from the main stream to the recirculation zones as demonstrated by Gonzalez and Chanson (2004a) with a 16º slope.

Observations from the sidewall showed some effects of the vanes on cavity recirculation. Vanes appeared to be subjected to strong pressure and shear forces. Fluctuations seemed to be of the same period and in phase with cavity fluid ejections as reported by Djenidi et al. (1999) for d-type roughness and Chanson et al. (2002) for stepped chute flows. Longitudinal troughs above the vanes were also observed, possibly associated with wakes and quasi-coherent low speed streaks immediately above each vane.

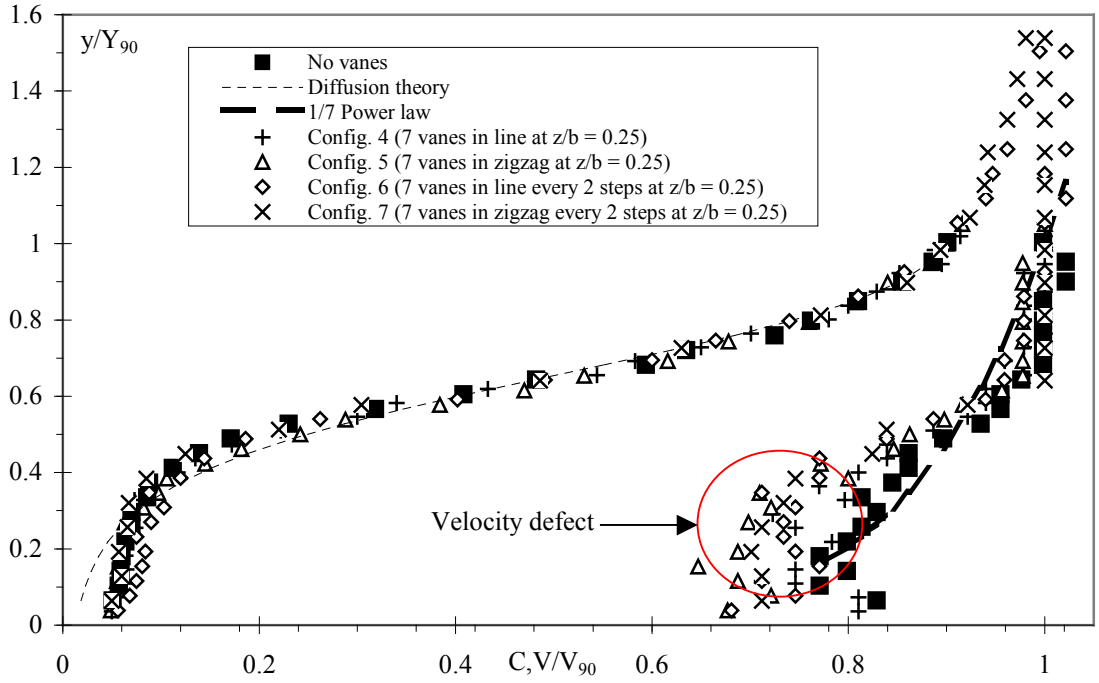

Fig. 3 Void fraction and velocity distributions at step edge 9 (d_c/h = 1.4, Re = 6.5 E+5) - Comparison between Config. 1 (No vane) and Configs. 4, 5, 6, & 7 (7 vanes) at z/b = 0.25

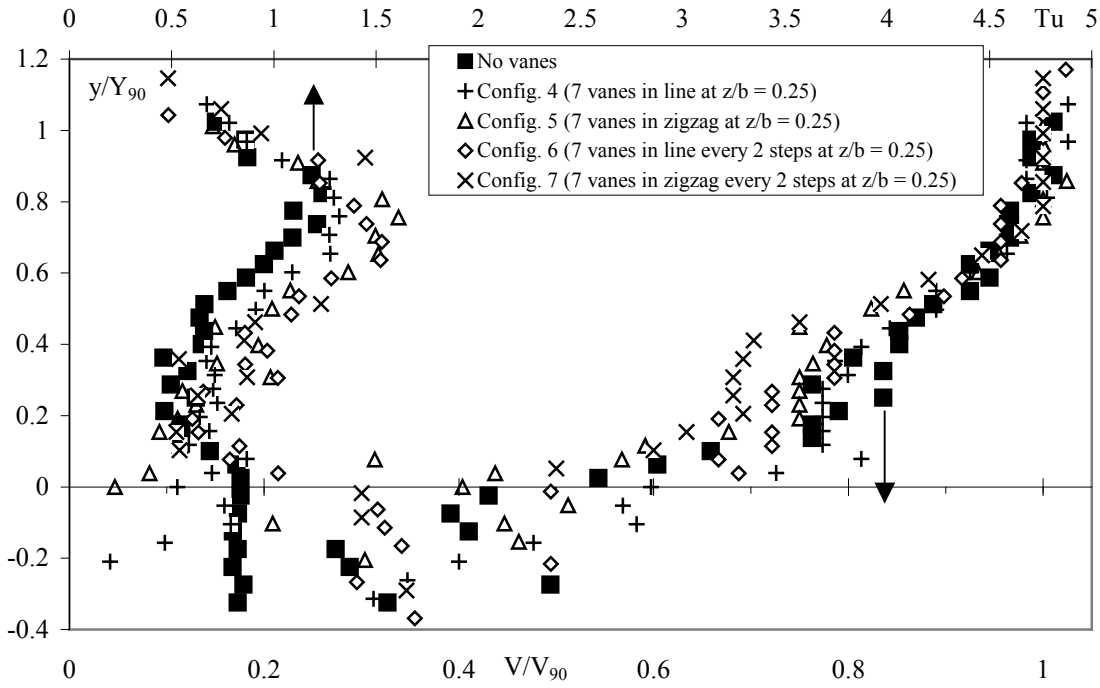

Fig. 4 Turbulence intensity and velocity distributions at one quarter of the distance between step edges 9 and 10 (d_c/h = 1.4, Re = 6.5 E+5) - Comparison between Configuration 1 (No vane) and configurations 4, 5, 6, & 7 (7 vanes) at z/b = 0.25 and $x/\sqrt{h^2+l^2}$ = 0.25

4. DETAILED AIR-WATER FLOW PROPERTIES

A detailed comparison of air-water flow properties was conducted for stepped configurations with vanes for data measured at three transverse locations z/b = 0, 0.25 and 0.5, where z is the transverse distance from the channel centreline and b is the spacing between vanes (Fig. 2). These results were compared with data for the stepped geometry without vanes (Configuration 1). Figure 3 presents typical results in terms of distributions of air concentration C and velocity V/V_{90} for configurations 4, 5, 6 and 7 at step edge 9 and z/b = 0.25, where y is the distance normal to the pseudo-bottom formed by the step edges, Y_{90} the distance where C = 0.90 and V_{90} is the air-water flow velocity at $y = Y_{90}$. In Figure 3, the void fraction distributions are compared with an analytical solution of the air bubble diffusion equation :

$$C = 1 - \tanh^2\left(K' - \frac{y'}{2 * D_o} + \frac{(y' - 1/3)^3}{3 * D_o}\right) \quad (1)$$

where $y' = y/Y_{90}$, and D_o and K' are dimensionless functions of the mean air concentrations only (Chanson and Toombes 2002). Also in Figure 3, the velocity data are compared with a 1/7-th power law.

Void fraction distributions, including data presented in Fig. 3, suggested negligible effects of the vanes on the void fraction distributions and on the rate of air entrainment. Velocity measurements at all transverse positions for each vane configuration showed a strong effect of the vanes on the flow for $y/Y_{90} < 0.5$ to 0.7. In presence of vanes, a velocity defect region was observed above the longitudinal ribs, suggesting a developing wake region above each vane.

The results demonstrated that the effect of the vanes was not limited to the cavity flow but extended into the mainstream. Fig. 4 presents dimensionless velocity V/V_{90} and turbulence level Tu distributions obtained for configurations 1, 4, 5, 6 and 7 between step edges 9 and 10 above the step cavity at z/b = 0.25. Results hinted that the streamwise effect of vanes was limited to one downstream cavity. No noticeable difference in terms of velocity and turbulence level distributions was observed between Configurations 1, 6 and 7 despite the presence of vanes in Configurations 6 and 7.

Turbulence level distributions showed high values for all investigated flow conditions. For the configurations with vanes, results obtained at step edges were similar, showing consistently higher turbulence levels than in absence of vanes (e.g. Fig. 4). Basically the presence of vanes induced an increase of turbulence by about 40%. Maximum turbulence levels were observed for the configurations 3 and 5: i.e., vanes in zigzag.

In highly turbulent skimming flows, probability distribution functions (PDF) of bubble chord sizes were systematically analysed for each configuration in the bubbly flow region (C < 0.3) while drop size distributions were studied in the spray region (C > 0.7). Fig. 5 presents typical bubbly flow results for identical configurations at locations below and above the pseudo-bottom with similar void fractions. In Fig. 5, the legend gives further details including the number of detected bubbles in a 20-s record. Overall, the results demonstrated a greater number of bubbles detected in the mainstream (y/h > 0) and a broader range of bubble sizes than at locations below the pseudo-bottom for an identical void fraction. For example, in Fig. 5, the amount of bubbles detected in the mainstream (Fig. 5B) were at least twice as much as that detected in the recirculation region (Fig. 5A), for locations with very-similar void fractions. Further the results (Fig. 5) suggested that the flow structure did not vary much for configurations 1, 2 & 3 (No vane, 3 vanes in line and 3 vanes in zigzag respectively). More the presence of vanes and the vane configurations had little effects on the streamwise structure of the flow (e.g. cluster index)

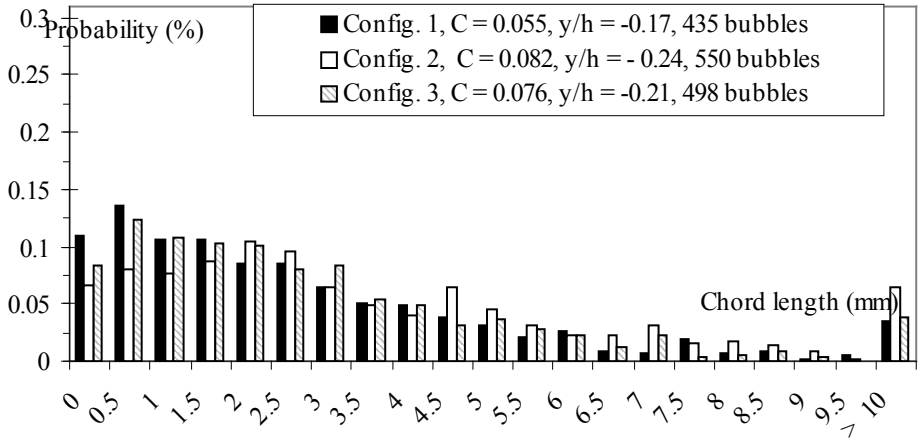

(A) Measurements below the pseudo-bottom (y/h < 0).

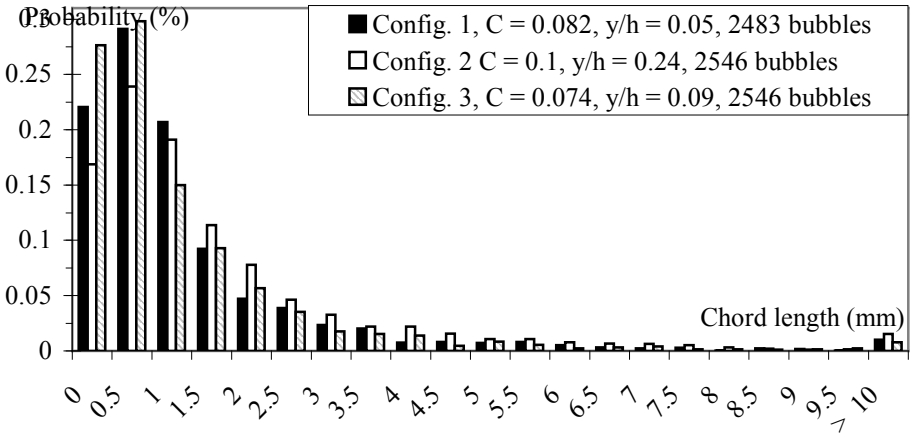

(B) Measurements in the free-stream flow above the pseudo-bottom (y/h > 0)

Fig. 5 Air-bubble chord length probability distributions function in the bubbly flow region (d_c/h=1.4, Re = 6.5 E+5, C < 0.3) between step edges 9 and 10 at $x/\sqrt{h^2+l^2}$ = 0.25 and z/b = 0.25

5. FLOW RESISTANCE AND ENERGY DISSIPATION

Flow resistance was calculated from the average friction slope S_f for all the configurations at z/b = 0 (above vanes), 0.25 and 0.5, using the approach of Chanson et al. (2002). Results are presented in terms of the Darcy friction factor f_e in Table 2 for all configurations, where :

$$f_e = \frac{8 * g}{q_w^2} * \int_{y=0}^{Y_{90}} (1 - C) * dy * S_f \quad (2)$$

q_w is the water discharge per unit width and g is the gravity constant. In Table 2, f_e is a longitudinal average friction factor at a dimensionless transverse location z/b. For configurations with vanes, the results were averaged transversally to yield a equivalent friction factor $\tilde{f}_e$ of the whole chute.

Overall, the experimental measurements yielded transverse-averaged Darcy friction factors $\tilde{f}_e$ of 0.16, 0.21, 0.21 and 0.20 in average for no vane, 3 and 7 vanes in line, and 7 vanes in line every 2 steps respectively (Configs. 1, 2, 4, 6 respectively). They implied friction factors of = 0.22, 0.22 and 0.21 in average for 3 and 7 vanes in zigzag, and 7 vanes in zigzag every 2 steps respectively (Configs. 3, 5, 7 respectively). Basically the findings suggested consistently that the presence of vanes increased the flow resistance and the rate of energy dissipation for the investigated flow conditions. Maximum values of equivalent Darcy friction factors were observed for configurations with vanes in zigzag (Configurations 3 and 5). Results for the configuration 6 and 7 (vanes every 2 steps) indicated systematically lower flow resistance with these configurations than with the other vane configurations.

The presence of vanes prevented the transverse development of large-scale turbulence in the cavities. It is believed that the inhibition of large transverse vortical structures was associated with enhanced vertical mixing between recirculation zones and mainstream. It is

suggested a modification of the mixing layer developing downstream of each step edge (Fig. 1), with a greater rate of expansion and larger transfer of momentum from the free-stream to the cavity flow in presence of vanes. Turbulent mixing enhancement was further associated with the development of streamwise coherent vortices in the main stream. Greater vertical mixing was also associated with greater spray generation in the configurations with vanes. Experimental data showed consistently that the dimensionless water flux for $0.90 \leq C \leq 0.99$ doubled in presence of vanes.

Table 2. Flow resistance estimates in air-water skimming flows without and with vanes at several transverse locations (z/b = 0, 0.25, 0.5)

d_c/h	f_e								
	Config. 1 No vane	Config. 2 3 vanes in line			Config. 3 3 vanes in zigzag		Config. 4 7 vanes in line		
		z/b=0	z/b=0.25	z/b=0.5	z/b=0.25	z/b=0.5	z/b=0	z/b=0.25	z/b=0.5
1.1	0.169	0.238	0.167	0.186	0.141	0.212	--	0.174	0.170
1.25	0.176	0.236	0.186	0.173	0.151	0.287	--	0.170	0.176
1.4	0.0924	0.311	0.145	0.133	0.207	0.288	0.281	0.165	0.166
1.5	0.211	0.271	0.191	0.258	0.225	0.227	--	0.170	0.163

d_c/h	Config. 5 7 vanes in zigzag		Config. 6 7 vanes in line every 2 steps			Config. 7 7 vanes in zigzag every 2 steps	
	z/b=0.25	z/b=0.5	z/b=0	z/b=0.25	z/b=0.5	z/b=0.25	z/b=0.5
1.1	0.180	0.238	0.216	0.177	0.181	0.165	0.2057
1.25	0.205	0.3112	0.258	0.167	0.191	0.120	0.236
1.4	0.211	0.249	0.266	0.163	0.160	0.136	0.231
1.5	0.215	0.170	0.373	0.121	0.163	0.207	0.346

6. CONCLUSION

Turbulence manipulation was investigated systematically in skimming flows down a stepped chute. The results were obtained in a large-size facility operating at large Reynolds numbers to minimise potential scale effects, discussed more thoroughly by Gonzalez and Chanson (2004b). New turbulence manipulation arrangements were tested and compared with the classical flat-step geometry. These consisted of triangular vane arrangements. Detailed air-water flow measurements demonstrated that the vanes influenced the air-water flow properties in both mainstream and recirculating regions. Maximum flow resistance was observed for configurations with vanes arranged in zigzag. Based upon present results, it is hypothesised that greatest interfacial aeration and air-water transfer rates can be achieved with vane configurations in zigzag placed at each step. It is also suggested that more intricate geometries (e.g. vanes in zigzag every 2 steps) will not further flow resistance. This study provides new information on the complex structure of highly turbulent aerated flows and suggests that turbulence manipulation can be applied to stepped spillways to enhance energy dissipation.

ACKNOWLEDGEMENTS

The writers acknowledge the helpful comments of Dr John Macintosh (Water Solutions) the technical assistance of Graham Illidge and Clive Booth (The University of Queensland).

The first writer thanks the financial support of the National Council for Science and Technology of Mexico (CONACYT).

REFERENCES

Andre, S., Boillat, J.L., Schleiss, A.J., and Matos, J. (2004). "Energy Dissipation and Hydrodynamic Forces of Aerated Flow over Macro-Roughness Linings for Overtopped Embankment Dams." *Proc. Intl Conf. on Hydraulics of Dams and River Structures*, Tehran, Iran, Balkema Publ., The Netherlands, pp. 189-196.

Chanson, H. (2001). "The Hydraulics of Stepped Chutes and Spillways." *Balkema*, Lisse, The Netherlands, 418 pages (ISBN 90 5809 352 2).

Chanson, H., and Gonzalez, C.A. (2004). "Stepped Spillways for Embankment dams: Review, Progress and Development in Overflow Hydraulics." *Proc. Intl Conf. on Hydraulics of Dams and River Structures*, Tehran, Iran, Balkema Publ., The Netherlands, pp. 287-294.

Chanson, H., and Toombes, L. (2002). "Air-Water Flows down Stepped chutes : Turbulence and Flow Structure Observations." *Intl Jl of Multiphase Flow*, Vol. 27, No. 11, pp. 1737-1761.

Chanson, H., Yasuda, Y., and Ohtsu, I. (2002). "Flow Resistance in Skimming Flows and its Modelling." *Can Jl of Civ. Eng.*, Vol. 29, No. 6, pp. 809-819.

Crowe, C., Sommerfield, M., and Tsuji, Y. (1998). "Multiphase Flows with Droplets and Particles." *CRC Press*, Boca Raton, USA, 471 pages.

Djenidi, L., Elavasaran, R., and Antonia, R.A. (1999). The Turbulent Boundary Layer over Transverse Square Cavities. *Jl Fluid Mech.*, Vol. 395, pp. 271-294.

Gonzalez, C.A. (2005)."An Experimental Study of Free-Surface Aeration on Embankment Stepped Chutes." *Ph.D. Thesis*, Dept. of Civil Engineering, University of Queensland, Brisbane, Australia.

Gonzalez, C.A., and Chanson, H. (2004a). "Interactions between Cavity Flow and Main Stream Skimming Flows: an Experimental Study." *Can Jl of Civ. Eng.*, Vol. 31, No. 1, pp. 33-44.

Gonzalez, C.A., and Chanson, H. (2004b). "Scale Effects in Moderate Slope Stepped Spillways. Experimental Studies in Air-Water Flows." *Proc. 8th National Conference on Hydraulics in Water Engineering*, IEAust., Gold Coast, Australia, H. Chanson and J. Macintosh Ed., 8 pages (CD-ROM).

Mochizuki, S., Izawa, A., and Osaka, H. (1996). "Turbulent Drag Reduction in a d-type Rough Wall Boundary Layer with Longitudinal Thin Ribs Placed within Traverse Grooves Higher-order Moments and Conditional Sampling Analysis)." *Trans. JSME Intl Journal*,series B, Vol. 39, No. 3, pp. 461-469.

Mossa, M., Yasuda, Y., and Chanson, H (2004). "Fluvial, Environmental and Coastal Developments in Hydraulic Engineering." *Balkema*, Leiden, The Netherlands, Proc. Intl Workshop on State-of-the-Art Hydraulic Engineering, 16-19 Feb. 2004, Bari, Italy, 248 pages (ISBN 04 1535 899 X).

Ohtsu, I., Yasuda, Y., and Takahashi, M. (2004). "Flow Characteristics of Skimming Flows in Stepped Channels." *Jl of Hyd. Engrg.*, ASCE, Vol. 130, No. 9, pp. 860-869.

Yasuda, Y., and Chanson, H. (2003). "Micro- and Macro-scopic Study of Two-Phase Flow on a Stepped Chute." *Proc. 30th IAHR Biennial Congress*, Thessaloniki, Greece, Vol. D, pp. 695-702.